Short communication

Exploring the mechanism of interaction between 5-(ethoxycarbonyl)-6-methyl-4-(4-methoxyphenyl)-3,4-dihydropyrimidin-2(1H)-one and human serum albumin: Spectroscopic, calorimetric and molecular modeling studies

Gongke Wang, Xiang Li, Xuelian Ding, Dongchao Wang, Changling Yan, Yan Lu*

School of Chemistry and Environmental Science, Key Laboratory of Green Chemical Media and Reactions, Ministry of Education, Henan Normal University, Xinxiang, Henan 453007, PR China

ABSTRACT

In this paper, binding interaction of 5-(ethoxycarbonyl)-6-methyl-4-(4-methoxyphenyl)-3,4-dihydropyrimidin-2(1H)-one (EMMD) with human serum albumin (HSA) under physiological conditions was investigated by using spectroscopy, isothermal titration calorimetry (ITC) and molecular modeling techniques. The results of spectroscopic studies suggested that EMMD have a strong ability to quench the intrinsic fluorescence of HSA through static quenching procedure. ITC investigations indicated that drug–protein complex was stabilized by hydrophobic forces and hydrogen bonds, which was consistent with the results of molecular modeling studies. Competitive experiments indicated the displacement of warfarin by EMMD, which revealed that the binding site of EMMD to HSA was located at subdomain IIA.

© 2011 Elsevier B.V. All rights reserved.

1. Introduction

Dihydropyrimidinones (DHPMs) and their derivatives are well known heterocyclic units in the realm of natural and synthetic organic chemistry due to their therapeutic and pharmacological properties. Furthermore, they have attracted considerable interest in recent years because of their medicinally importance as calcium channel blockers [1], antihypertensive agents [1], α1a- antagonists [2], mitotic kinesin Eg5 inhibitors [3], melanin concentrating hormone receptor antagonists [4], neuropeptide antagonists [5,6] and strong resistance HIVgp120-CD4 function [7]. Moreover, several alkaloids containing DHPMs as a core unit have been isolated from marine source, which also showed interesting biological properties. As a member of the derivatives of DHPMs, 5-(ethoxycarbonyl)-6-methyl-4-(4-methoxyphenyl)-3,4-dihydropyrimidin-2(1H)-one (EMMD, structure shown in Fig. 1) is regarded as the potential new protein targeted drug, which brings its wide applicability in biochemistry and biomedicine.

Human serum albumin (HSA) has two primary binding sites, site I and site II, which are hydrophobic cavities located in subdomain IIA and subdomain IIIA respectively. Most compounds bind to the two sites with an affinity constant of 10^4–10^6 M^{-1} [8]. The remarkable binding properties of HSA account for the central role in both the efficacy and rate of delivery of drugs. Therefore, the studies on the binding of drugs to HSA become an important research field in chemistry, life science and clinical medicine. Recently, extensive investigations into the interaction between HSA and internal compounds or pharmaceutical molecules have been performed [9,10], but the binding interaction of HSA with DHPMs derivatives has seldom been reported.

In this work, the mechanism and characteristics of interaction between EMMD and HSA were investigated systematically by spectroscopic, calorimetric and molecular modeling methods for the first time. We hope that this study will be helpful for realizing the distribution and transportation of drugs in vivo, elucidating the action mechanism, toxicity and dynamics of drugs at the molecular level.

2. Materials and methods

EMMD was successfully synthesized by the literature procedure [11], HSA (66,000 Da) and warfarin were purchased from Sigma Chemical Company (USA). 0.1 M Tris–HCl buffer solution (containing 0.1 M NaCl) was used to keep the pH of the solutions at 7.40. All other chemicals were of analytical grade and used without further purification.

* Corresponding author. Tel.: +86 373 3325249; fax: +86 373 3325249.
E-mail addresses: yanlu2001@sohu.com, wanggongke@126.com (Y. Lu).
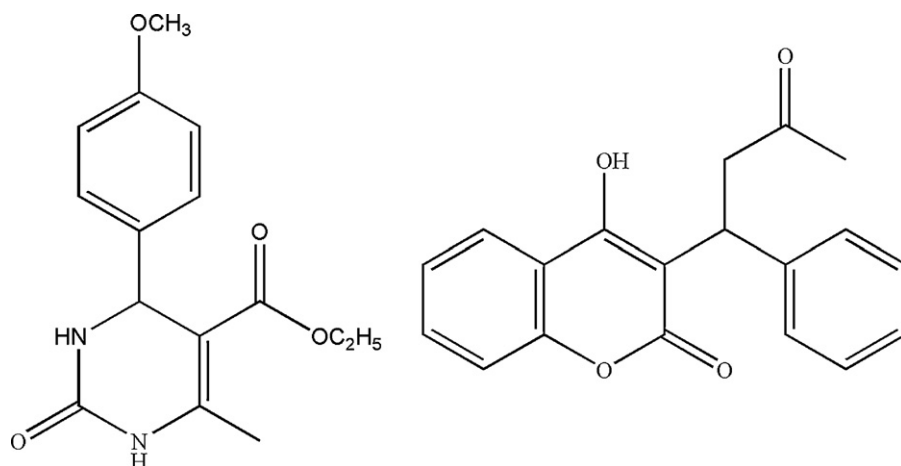
Fig. 1. The chemical structure of EMMD and warfarin.

The UV-absorption spectroscopy was performed on a TU-1810 UV spectrophotometer (Puxi Analytic Instruments Co., LTD, China) equipped with 1.0 cm quartz cells at 25 °C. The fluorescence quenching of HSA with increasing concentration of EMMD was recorded on a Cary Eclipse fluorescence spectrophotometer (Varian, America) with 5 nm/5 nm slit widths using an excitation wavelength of 280 nm. The fluorescence titration data were analyzed by the Stern–Volmer equation [10,12]:

$$\frac{F_0}{F} = 1 + K_{sv}[Q] \tag{1}$$

where F_0 and F represent the steady-state fluorescence intensities in the absence and presence of quencher, respectively, and [Q] is the concentration of quencher. K_{sv} is the Stern–Volmer quenching constant, which was determined by linear regression of a plot of F_0/F versus [Q]. The binding constants between HSA and EMMD at different temperatures were determined by the modified Stern–Volmer equation [13]:

$$\frac{F_0}{\Delta F} = \frac{1}{f_a K_a} \frac{1}{[Q]} + \frac{1}{f_a} \tag{2}$$

In the present case, ΔF is the difference in fluorescence in the absence and presence of the quencher, f_a is the fraction of accessible fluorescence and K_a is the equilibrium binding constant.

Isothermal titration calorimetry (ITC) was performed using a Model Nano-ITC 2G biocalorimetry instrument (TA, USA) at 25 °C. HSA and EMMD solutions were properly degassed prior to the titrations to avoid the formation of bubbles in the calorimeter cell. In the titration, HSA was titrated by EMMD with 25 successive injections of 10 μL each at intervals of 400 s. Fitting the data according to the independent model resulted in the stoichimetry (n), equilibrium binding constant (K_b), and enthalpy of complex formation (ΔH^0). The other thermodynamic parameters were calculated by the following formulas:

$$\Delta G^0 = -RT \ln K_b \tag{3}$$

$$\Delta G^0 = \Delta H^0 - T \Delta S^0 \tag{4}$$

The crystal structure of HSA was taken from the Brookhaven Protein Data Bank (entry codes 1h9z). The potential of the 3D structure of HSA was assigned according the Amber 4.0 force field with Kollman-all-atom charges. The initial structure of all the molecules was generated by molecular modeling software Sybyl 6.9.1. The geometries of the ligand molecules were optimized using the Tripos force field with Gasteiger–Hückel charges. FlexX program was applied to calculate the possible conformations of the ligand that bind to protein.

3. Results and discussion

3.1. Fluorescence quenching of HSA by EMMD

Fluorescence spectroscopy was used to characterize the binding properties of the chromophore with other molecules [14]. The effect of EMMD on HSA fluorescence spectroscopy at 25 °C is shown in Fig. 2. It is seen from Fig. 2 that the fluorescence intensity of HSA at 345 nm decreased gradually, and a slight blue shift was observed with the addition of EMMD when the concentration of HSA was fixed. These observations may be referred to a strong binding of EMMD to HSA [15]. Additionally, it implies that the conformational changes of HSA are induced by EMMD under the conditions and the chromophore of HSA (Trp214) may be placed in a more hydrophobic environment [10].

3.2. Quenching mechanism and binding constants

The Stern–Volmer plots of EMMD with HSA at different temperatures were constructed by using equation (1), and the best linear fits to the data resulted in the Stern–Volmer quenching constant K_{sv} 2.31×10^5 M^{-1}, 2.12×10^5 M^{-1} and 2.03×10^5 M^{-1} at 15 °C, 25 °C

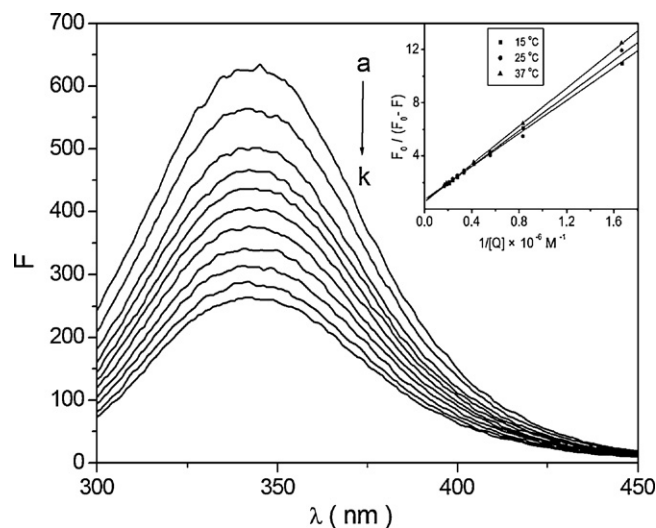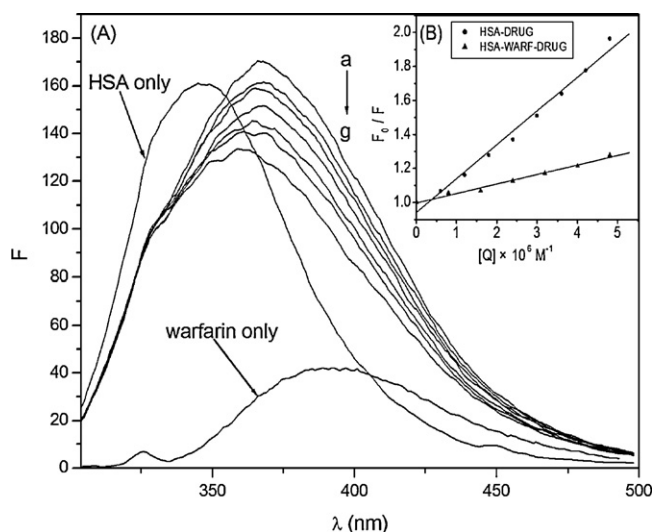**Fig. 2.** Effect of EMMD on quenching of HSA fluorescence. c_{HSA} = 3 μM; from a to k: c_{drug} = 0, 0.6, 1.2, 1.8, 2.4, 3.0, 3.6, 4.2, 4.8, 5.4 and 6.0 μM, respectively (pH = 7.4, T = 25 °C, λ_{ex} = 280 nm). Inset: the modified Stern–Volmer plots for the binding of EMMD to HSA at different temperatures.

Fig. 3. (A) Effect of EMMD on the quenching of warfarin–HSA complex fluorescence. From a to g: $c_{HSA} = c_{warfarin} = 2\,\mu M$, $c_{EMMD} = 0$, 0.8, 1.6, 2.4, 3.2, 4.0, 4.8 μM; (B) The Stern–Volmer curves for the binding of EMMD to HSA (filled circle) and warfarin–HSA complex (filled triangle). pH = 7.4, $T = 37\,°C$, $\lambda_{ex} = 295$ nm.

Fig. 4. The integrated ITC curve of EMMD binding to HSA according to the independent binding model at 25 °C. The initial concentration of EMMD is 1.0 mM and the concentration of HSA is 0.1 mM.

and 37 °C, respectively. We can see that K_{sv} is inversely correlated with temperature, which suggests that the probable quenching mechanism is initiated by the complex formation rather than by the dynamic collision.

In order to further confirm the quenching mechanism, the absorption spectra of HSA and the difference absorption spectra between HSA–EMMD and EMMD at the same concentration were employed. The results show that the absorption spectra of HSA and the difference absorption spectra between HSA–EMMD complex and EMMD can not be superposed within experimental error. Therefore, it is reconfirmed that the probable quenching mechanism of EMMD with HSA is a static quenching procedure of ground-state complex formation.

The dependence of $F_0/\Delta F$ on the reciprocal value of the quencher concentration $[Q]^{-1}$ (inset, Fig. 2) illustrates that the quenching of EMMD to HSA is in good agreement with the modified Stern–Volmer equation (Eq. (2)). Herein, the values of binding constant K_a were determined as $1.15 \times 10^5\,M^{-1}$, $0.88 \times 10^5\,M^{-1}$ and $0.71 \times 10^5\,M^{-1}$ at 15 °C, 25 °C and 37 °C, respectively. It is found that EMMD can effectively bind to HSA. At the same time, it shows that the binding constants decrease with the increase of temperatures, resulting in the reduction of the stability of the EMMD–HSA complex.

3.3. Identification of the binding site of EMMD on HSA

Warfarin and ibuprofen were used as site marker fluorescence probes for monitoring site I and site II of HSA, respectively [16]. To identify the binding site of EMMD on the region of HSA, the site marker competitive experiments were employed by using warfarin which specifically binds to a known site on HSA. In the site marker competitive experiment, EMMD was gradually added to the solution of HSA–warfarin complex. As displayed in Fig. 3A, with addition of warfarin to HSA, the maximum emission wavelength of HSA had an obvious red shift and the fluorescence intensity was higher than that without warfarin. Then the titration of HSA–warfarin complex with EMMD, the fluorescence intensity decreased gradually, accompanied by a blue shift of maximum emission wavelength (from 366 to 359 nm). The quenching constants of EMMD with HSA in the absence and presence of warfarin were analyzed by the Stern–Volmer plots (Fig. 3B), which were
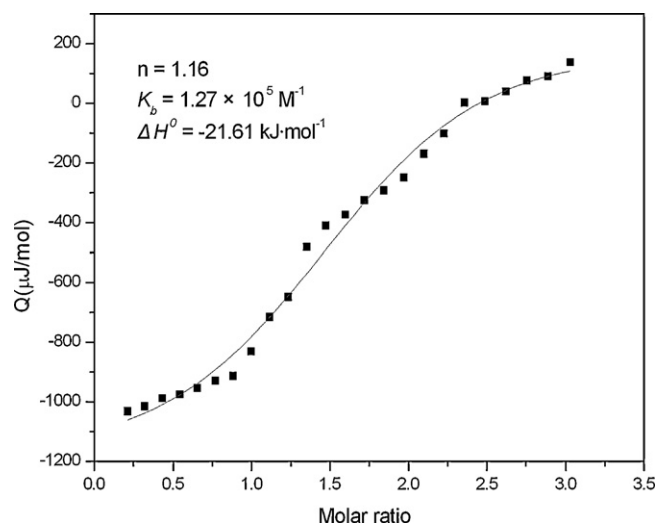
calculated as $2.1 \times 10^5\,M^{-1}$ and $0.56 \times 10^5\,M^{-1}$, respectively. The results show that the quenching constant obviously decreased in the presence of warfarin. This may be due to that warfarin prevents the binding of EMMD to HSA in its usual binding site. The blue shift of maximum wavelength suggests that the hydrophobicity of the region surrounding site I is increased, and indicates that bound EMMD to HSA is distinctly affected by adding warfarin. A reasonable explanation is that the bound warfarin fell out of the binding site and displaced by EMMD. So, it can be confirmed that EMMD binds to site I (subdomain IIA of HSA) with high affinity, which is in accordance with the molecular modeling studies below.

3.4. ITC studies

ITC has become an effective tool to thermodynamically characterize the binding of small molecules to macromolecules [17]. Further, it provides significant insight into the energetics in complex formation. Therefore, this technique was used to thermodynamically characterize the formation of EMMD–HSA complex. Fig. 4 shows the integrated heats of reaction plotted against mole ratio of EMMD to HSA after the correction for dilution effects of EMMD. The data points reflect the experimental points while the continuous line represents the calculated fits of the data. The binding was characterized by exothermic heats. The binding constant and thermodynamic parameters of EMMD–HSA complex, estimated by fitting the integrated heats according to the independent binding model, are K_b $1.27 \times 10^5\,M^{-1}$, $\Delta H^0 = -21.61$ kJ mol^{-1} and $n = 1.16$, respectively. According to Eqs. (3) and (4), the other thermodynamic parameters were evaluated as $\Delta G^0 = -29.13$ kJ mol^{-1} and $\Delta S^0 = 25.22$ J mol^{-1} K^{-1}. We can see that the binding constant K_b determined here is approximately consistent with the result of fluorescence titration. Additionally, it is found that the enthalpy term (-21.61 kJ mol^{-1}) is near the free energy (-29.13 kJ mol^{-1}), which indicates that the binding is predominantly enthalpy driven. Additionally, the negative enthalpy and the positive entropy suggest that hydrophobic interactions and hydrogen bonds may play a major role in the binding of EMMD to HSA [18].

3.5. Molecular modeling studies

In addition to providing experimentally originated spectroscopic and thermodynamic parameters, we also applied the
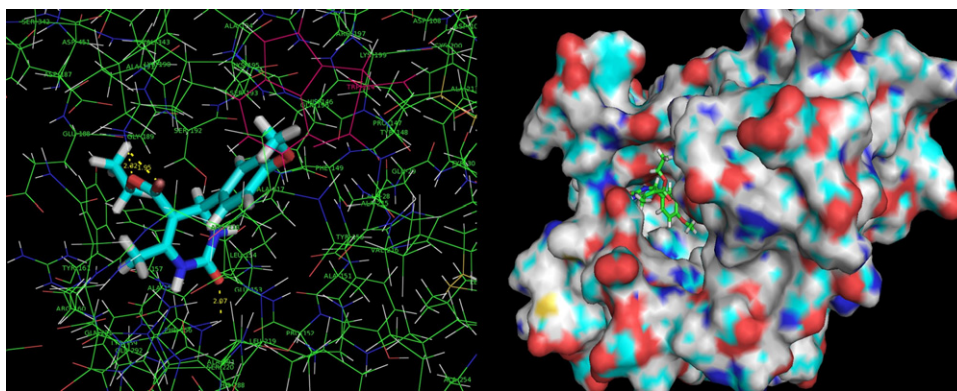
Fig. 5. Interaction mode between EMMD and HSA, only residues around 6 Å of the ligand are displayed. The residues of the HSA are presented using line in (left panel) and the surface of the HSA is displayed by QUICK method in (right panel). The ligand structure is represented using stick model. The hydrogen bonds between EMMD and HSA are represented using yellow dashed line.

molecular modeling methodology, which offers a molecular level explanation with the ability to estimate the participation of specific chemical groups and their interactions in complex stabilization [19].

The optimum binding mode between EMMD and HSA was presented in Fig. 5. From Fig. 5 (right panel), we can see that EMMD can bind to a hydrophobic pocket of HSA. In addition, as shown in Fig. 5 (left panel), EMMD is located within the binding pocket of subdomain IIA of HSA (the warfarin binding pocket). Furthermore, docking of EMMD to HSA creates a hydrophobic environment near Trp214, which provides a good structural basis to explain the efficient fluorescence quenching of HSA in the presence of EMMD. On the other hand, there are hydrogen interactions of atoms O and H of EMMD with the residues Lys195, His288, and Lys195 of HSA. The length of the hydrogen bond is, respectively, 2.07 Å, 1.95 Å, and 2.32 Å. The results demonstrate that the formation of hydrogen bond decreases the hydrophilicity and increases the hydrophobicity to stabilize the EMMD–HSA system. Therefore, the results obtained from molecular modeling suggest that the interaction between EMMD and HSA is dominated by hydrophobic force and hydrogen bonds, which well agree with ITC studies described above.

4. Conclusions

The binding interaction of EMMD with HSA has been investigated by using different spectral, ITC and molecular modeling techniques. The experimental results suggested that EMMD could bind to HSA through a static quenching procedure. The hydrophobic interaction and hydrogen bonds played a major role in the reaction. It is noted that the binding site was located in the hydrophobic pocket of subdomain IIA according to the competitive binding experiment and molecular modeling studies. We hope that this work can provide important insight into the interactions of the DHPMs derivatives with physiologically important HSA. Furthermore, the results are helpful for the further research in the rational design of this series of compounds.

References

[1] C.O. Kappe, W.M. Fabian, M.A. Semones, Conformational analysis of 4-aryl-dihydropyrimidine calcium channel modulators. A comparison of ab initio, semiempirical and X-ray crystallographic studies, Tetrahedron 53 (1997) 2803–2816.

[2] D. Nagarathnam, S.W. Miao, B. Lagu, G. Chiu, J. Fang, T.G. Murali Dhar, et al., Design and synthesis of novel α1a adrenoceptor-selective antagonists. 1. Structure-activity relationship in dihydropyrimidinones, J. Med. Chem. 42 (1999) 4764–4777.

[3] S.J. Haggarty, T.U. Mayer, D.T. Miyamoto, R. Fathi, R.W. King, T.J. Mitchison, S.L. Schreiber, Dissecting cellular processes using small molecules: identification of colchicine-like, taxol-like and other small molecules that perturb mitosis, Chem. Biol. 7 (2000) 275–286.

[4] S Lou, P. Dai, S.E. Schaus, Asymmetric mannich reaction of dicarbonyl compounds with α-amido sulfones catalyzed by cinchona alkaloids and synthesis of chiral dihydropyrimidones, J. Org. Chem. 72 (2007) 9998–10008.

[5] K.S. Atwal, G.C. Rovnyak, B.C. O'Reilly, J. Schewartz, Substituted 1,4-dihydropyrimidines. 3. Synthesis of selectively functionalized 2-hetero-1,4-dihydropyrimidines, J. Org. Chem. 54 (1989) 5898–5907.

[6] K.S. Atwal, G.C. Rovnak, S.D. Kimballs, D.M. Floyd, S. Moreland, B.N. Swanson, et al., Dihydropyrimidine calcium channel blockers. II. 3-Substituted-4-aryl-1,4-dihydro-6-methyl-5-pyrimidinecarboxylic acid esters as potent mimics of dihydropyridines, J. Med. Chem. 33 (1990) 2629–2635.

[7] A.D. Patil, N.V. Kumar, W.C. Kokke, M.F. Bean, A.J. Freyer, C.D. Brosse, et al., Novel alkaloids from the spone batzalla sp.: Inhibitors of HIV gp120-Human CD4 binding, J. Org. Chem. 60 (1995) 1182–1188.

[8] X.M. He, D.C. Carter, Atomic structure and chemistry of human serum albumin, Nature 358 (1992) 209–215.

[9] S.N. Khan, B. Islam, R. Yennamalli, A. Sultan, N. Subbarao, A.U. Khan, Interaction of mitoxantrone with human serum album: spectroscopic molecular modeling studies, Eur. J. Pharm. Sci. 35 (2008) 371–382.

[10] Y.J. Hu, Y. Liu, X.H. Xiao, Investigation of the interaction between berberine and human serum albumin, Biomacromolecules 10 (2009) 517–521.

[11] N.S. Nandurkar, M.J. Bhanushali, M.D. Bhor, B.M. Bhanage, Y(NO₃)₃·6H₂O: a novel and reusable catalyst for one pot synthesis of 3,4-dihydropyrimidin-2(1H)-ones under solvent-free conditions, J. Mol. Catal. A 271 (2007) 14–17.

[12] Q.J. Zhou, J.F. Xiang, Y.L. Tang, J.P. Liao, C.Y. Yu, H. Zhang, et al., Investigation on the interaction between a heterocyclic aminal derivative, SBDC, and human serum albumin, Colloids, Surf. B Biointerfaces 61 (2008) 75–80.

[13] S.S. Lehrer, Solute perturbation of protein fluorescence. The quenching of tryptophyl fluorescence of model compounds and of lysozyme by iodide ion, Biochemistry 10 (1971) 3254–3263.

[14] N.K. Modukuru, K.J. Snow, B.S. Perrin Jr., J. Thota, C.V. Kumar, Contributions of a long side chain to the binding affinity of an anthracene derivative to DNA, J. Phys. Chem. B 109 (2005) 11810–11818.

[15] S. Deepa, A.K. Mishra, Fluorescence spectroscopic study of serum albumin–bromadiolone interaction: fluorimetric determination of bromadiolone, J. Pharm. Biomed. Anal. 38 (2005) 556–563.

[16] Z.D. Qi, Y. Zhang, L.F. Liao, Y.W. Ou-Yang, Y. Liu, X. Yang, Probing the binding of morin to human serum albumin by optical spectroscopy, J. Pharm. Biomed. Anal. 46 (2008) 699–706.

[17] R. O'Brien, I. Haq, in: J.E. Ladbury, M. Doyle (Eds.), Biocalorimetry 2: Applications of Calorimetry in the Biological Sciences, John Wiley and Sons, West Sussex, England, 2004, pp. 3–34.

[18] Y.Y. Yue, X.G. Chen, J. Qin, X.J. Yao, A study of the binding of C.I. Direct Yellow 9 to human serum albumin using optical spectroscopy and molecular modeling, Dyes Pigments 79 (2008) 176–182.

[19] P. Górnas, G. Neunert, K. Baczyński, K. Polewski, Beta-cyclodextrin complexes with chlorogenic and caffeic acids from coffee brew: spectroscopic, thermodynamic and molecular modelling study, Food Chem. 114 (2009) 190–196.